To cite this version : Dang, Dinh Khanh and Mifdaoui, Ahlem *Performance optimization of a UWB-based network for safety-critical avionics.* In: The 19th IEEE International Conference on Emerging Technologies and Factory Automation (ETFA'2014), 16 September 2014 - 19 September 2014 (Barcelona, Spain)

Performance Optimization of a UWB-based Network for Safety-Critical Avionics

Dinh-Khanh Dang, Ahlem Mifdaoui
University of Toulouse-ISAE
dinh-khanh.dang@isae.fr, ahlem.mifdaoui@isae.fr

***Abstract*—To reduce the aircraft weight and maintenance costs while guaranteeing system performance and reliability, an alternative avionic communication architecture based on Ultra Wide Band (UWB) and TDMA protocol is proposed to replace the back-up part of safety-critical avionics network. The analysis and performance optimization of such a proposal is tackled as follows. First, appropriate system modeling and timing analysis, using Network Calculus and Integer Linear Programing (ILP) approach, are provided to evaluate the end-to-end delays and verify system predictability. Then, an optimization approach to find the optimal TDMA cycle duration, which minimizes the end-to-end delays, is proposed. Finally, the efficiency of our proposal to enhance the system performance is validated through a realistic avionic case study.**

I. Introduction

The inherent complexity of the avionic communication architecture is increasing due to the growing number of inter-connected end-systems and the expansion of exchanged data. This complexity leads to significant quantities of wires and connectors, and consequently increases weight and integration costs. Furthermore, avionic interconnects are still subject to structural failure and fire hazard, which decrease reliability and ramify maintenance efforts.

With the technological progress of wireless technologies, an alternative avionic communication architecture based on wireless connectivity is proposed to cope with these emerging issues. Wireless technology becomes a cost effective solution due to its ubiquity, simplicity and maturity. Moreover, using wireless technologies in the specific area of avionics brings significant advantages, such as quick installation and maintenance, reduced weight and suitable communication patterns for avionics, e.g., multicast. At the beginning step, the new UWB-based network is proposed to replace the back-up part of safety-critical avionics network. However, to guarantee hard real-time requirements of avionics, interesting challenges remain due to the non deterministic behavior of wireless communication and its sensitivity to interference and jamming.

In [5], the authors identified the main challenges when using wireless technologies in avionics. Then, an assessment of Commercial Off The Shelf (COTS) wireless technologies versus avionic requirements was conducted; and Ultra WideBand (UWB) [1] was selected as the most appropriate technology for critical avionic applications because of its high data rate, contention-free access protocol and high security mechanisms. Afterwards, in [6], the design of a new avionics network based on UWB [1] technology was proposed with Time Division Multiple Access (TDMA) as the arbitration protocol to guarantee timely communications, and diversity mechanisms, e.g., time and frequency, to guarantee reliability requirements. Then, the relevant aspects of such a proposal and analytical evaluation based on Network Calculus [10], offered guarantees in terms of predictability and reliability as investigated in the case of a single cluster avionics network.

To increase system scalability, i.e., increasing the number of interconnected end-systems, the proposed avionic wireless network has to be extended to a multi-cluster network where each cluster is based on the TDMA protocol. This multi-cluster wireless network will introduce at the same time multi-hop communications which may increase the delays. This fact has to be taken into account during timing analyses to verify the system schedulability. Furthermore, the selection of TDMA parameters of each cluster, i.e., slots and cycle lengths, has to be carefully conducted to guarantee the system's requirements in terms of predictability.

The contributions of this work are: (i) the design of a multi-cluster wireless network as an alternative avionics network to enhance system's scalability; (ii) an appropriate timing analysis, integrating refined models using Network Calculus and Integer Linear Programing (ILP), to evaluate the impact of multi-hop communications on end-to-end delays; (iii) an adequate optimization approach to find the optimal TDMA cycle duration of each cluster to minimize end-to-end delay; (iv) the validation of such a timing analysis in the case of a realistic avionics network, interconnecting more than 50 end-systems that send a total of more than 200 different multicast flows. The efficiency of our proposal to enhance the system performances is shown.

In the next section, we review the most relevant approaches in the area of timing analysis and performance optimization of TDMA-based wireless network. Afterwards, the design, analysis and performance optimization of our proposal is tackled as follows. First, the description of an alternative multi-cluster wireless network is presented in Section III. Then, system modeling and end-to-end delay analysis are detailed in Sections IV and V. Afterwards, the optimization approach of the TDMA cycle duration is explained in Section VI. Finally, in Section VII, the efficiency of our proposal to enhance system performances is illustrated within a realistic avionic application.

II. Related Work

The timing analysis of TDMA-based network using Network Calculus aims to provide a method to compute end-to end delay bounds of transmitted messages. These bounds are then compared with respective message deadlines to verify system schedulability. The advantages of using the Network Calculus theory are mainly its high scalability in case of multi-hop communication and its adaptability to handle the different service policies.

In [8] [9], the authors applied Network Calculus to provide real-time guarantees for Wireless Sensor Networks (WSNs). The former work proposed an optimization approach to design a TDMA arbiter for generic sink-tree WSNs; whereas the latter focused on performance analysis of such networks considering the sink mobility. In [12], the authors presented an approach to find the optimal cycle length as well as the minimum required bandwidth of a TDMA resource. These different approaches are based on a fluid flow model which may lead to optimistic end-to-end delays compared with a packet flow model, which is more appropriate to integrate the non-preemptive message transmission. Moreover, these were applied in the case of error-free environments for a single TDMA-based cluster. Hence, these approaches are not directly applicable in our considered case.

In our previous work [6], we proposed extended Network Calculus models to integrate the impact of non-preemption of message transmission under First In First Out (FIFO) and Fixed Priority (FP) policies, and transmission errors in the case of a single TDMA-based cluster. In this paper, we provide refined models based on Network Calculus and ILP, using the same idea introduced in [3] for tandem networks under FIFO multiplexing. This refined model allows us to compute tighter end-to-end delay bounds in the case of a multi-cluster TDMA-based network. Furthermore, the optimization of the TDMA cycle duration of each cluster is proposed to minimize the end-to-end delays. Finally, the efficiency of our proposed models to enhance system performances is validated through a realistic avionics network.

III. UWB FOR SAFETY-CRITICAL AVIONICS

In this section, three items are defined: the topology of the proposed wireless backup network, the tuning process of the MAC layer to guarantee timely communications and the choice of adequate reliability mechanisms.

A. Hybrid Architecture UWB/ Switched Ethernet

Avionics end-systems are concentrated in two avionics bays at the head of the aircraft, where the area of each avionics bay is less than a 6m-diameter circle. Our proposed architecture is based on clustering end-systems where each cluster is based on the UWB technology and a reserved band to avoid interference with the others. Hence, the achieved rate within each cluster in a range of 6 meters is about 200 Mbps. Furthermore, each cluster has a fully-connected topology which guarantees single hop intra-cluster communications.

The inter-cluster communication is handled by specific gateways where the communication patterns between gateways can be unicast, multicast or broadcast. A hybrid architecture based on a Full Duplex Switched Ethernet at 1Gbps to interconnect the clusters is proposed. An example of this architecture is shown in Fig. 1. A central switch is used to connect the gateways, and each gateway can immediately transmit its messages to the switch, to be then relayed to the final destination(s). Hence, this design allows high rate, deterministic and reliable communication. This hybrid architecture guarantees a high system scalability since additional avionics bays in the middle or in the back of the plane can be easily interconnected.

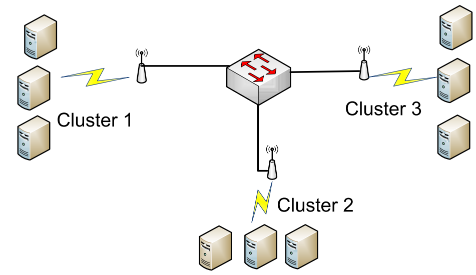

Figure 1: Example of Avionics Network with Hybrid Architecture

The gateways and the switch in this hybrid architecture have key functions. Each gateway has to convert the received UWB frames from any end-system in its associated cluster to Ethernet frames that will be transmitted to the Ethernet switch. Hence, to keep the end-to-end communication transparency, each gateway proceeds as follows. Each received UWB packet from an end-system in the associated cluster is encapsulated in an Ethernet frame (with respect to the minimal and maximal allowed sizes), and it is then transmitted to the Ethernet switch. Each received Ethernet frame from the Ethernet switch is decapsulated to extract the UWB packet to be then transmitted to the final destination. All frames are transmitted to the Ethernet switch following a FIFO policy.

The Ethernet Switch is an active device that identifies the destination port of an incoming packet and relays it to the specific port. If multiple packets have the same destination port, buffers are used to solve the problem of collision. This switch is a Store and Forward device that for safety reasons does not forward corrupted packets. FIFO is used to forward packets at the switch output port.

B. Tuning MAC protocol for Predictability Requirement

The classic superframe format of the UWB may imply a long synchronization phase and long transmission delays, which are unsuitable for avionic applications with short deadlines ranging from 2 to 128 ms. Hence, slot allocation and the TDMA cycle duration must be carefully configured, since they must efficiently handle different types of traffic and guarantee different temporal constraints. The modified superframe, as shown in Fig. 2, is constructed based on the following assumptions: (i) since all generated messages are known a priori, the slot allocation mechanism is configured off-line and will be followed in a static manner by all end-systems during the network deployment; (ii) during each superframe, the allocated time slot for each end-system is fixed and has a defined duration that depends on its generated traffic. Hence, the time slots are not equally allocated to the different end-systems, and the number of slots during a superframe depends on the number of end-systems.

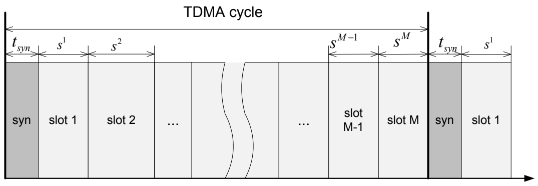

Figure 2: Modified UWB Superframe

C. Integrated Reliability Mechanisms

To integrate the multicast communication pattern required by avionic applications, the classic reliability mechanisms based on retransmissions and acknowledgments are disabled. The required reliability is guaranteed due to time and frequency diversity mechanisms, which are more adequate in an avionics context because of good properties of UWB technology and low fade margins. Furthermore, to avoid interference and jamming risks, adequate electromagnetic shielding solutions have to be implemented. The geographical concentration of end-systems in a short range of 6 meters facilitates the isolation of the backup network by using various methods described in [11], e.g., painting and lightweight anechoic chamber. Due to these different reliability mechanisms, bursty packet errors are avoided and the Packet Error Rate (PER) can be decreased to achieve the required level.

IV. System Modeling

In this section, the system modeling to evaluate the upper bounds on end-to-end delay for intra-cluster and inter-cluster traffic, illustrated in Fig. 3, is detailed. First, we review the basic Network Calculus concepts and the sufficient schedulability test. Next, we explain the traffic model to define the input arrival curve of the traffic. Then, the refined models of end-systems and TDMA protocol using Network Calculus and ILP are detailed to obtain the corresponding service curves. Afterwards, the service curves of the gateways and the Ethernet switch are presented.

A. Network Calculus Concepts

The worst-case performance analysis of our proposed network in this paper is based on *Network Calculus* theory [10], adapted to controlled traffic sources, and providing maximal bounds on delays and backlogs.

Delay bounds depend on the traffic arrival described by the so called *arrival curve* α, and on the availability of the traversed node described by the so called minimum *simple or strict service curve* β. The definitions of these considered curves are explained as following.

Definition 1. *(Arrival Curve) a function α is an arrival curve for a data flow with an input cumulative function R, such that $R(t)$ is the number of bits received until time t, iff:*

$$\forall t, s \geq 0, s \leq t, R(t) - R(s) \leq \alpha(t-s)$$

Definition 2. *(Simple service curve) The function β is the minimum simple service curve for a data flow with an input cumulative function R and output cumulative function R^* iff:*

$$R^* \geq R \otimes \beta$$

where $(f \otimes g)(t) = \inf_{0 \leq s \leq t}\{f(t-s) + g(s)\}$

Definition 3. *(Strict service curve) The function β is the minimum* strict *service curve for a data flow with an input cumulative function R and output cumulative function R^*, if for any backlogged period $]s,t]$*[1]*, $R^*(t) - R^*(s) \geq \beta(t-s)$.*

The delay bound D is the maximum horizontal distance between α and β called $h(\alpha, \beta)$; whereas the backlog bound B is the maximum vertical distance called $v(\alpha, \beta)$. The output arrival curve α^*, constrained by α at the input and under a maximum delay D, where $\alpha^*(t) = \alpha(t+D)$.

Finally, in order to compute delay bounds of individual traffic flows, we need the residual service curve according to the following theorem.

Theorem 1. *(Residual service curve - Blind Multiplex) [2] let f_1 and f_2 be two flows crossing a server that offers a* strict *service curve β such that f_1 is α_1-constrained, then the residual service curve offered to f_2 is:*

$$\beta_2 = (\beta - \alpha_1)_\uparrow$$

where $f_\uparrow(t) = \max\{0, \sup_{0 \leq s \leq t} f(s)\}$

B. Sufficient Schedulability Test

Using Network Calculus, an upper bound on end-to-end delay of each transmitted message m, D_m^{eed}, is computed and then compared to its respective temporal deadline, Dl_m. Hence, this schedulability test results in a sufficient but not necessary condition due to the pessimism introduced by the upper bounds. Nevertheless, we can still infer the traffic schedulability as follows:

$$\forall m \in messages,$$

$$D_m^{eed} \leq Dl_m \Longrightarrow \text{The } messages \text{ set is schedulable}$$

To compute upper bounds on end-to-end delays of transmitted messages using Network Calculus, we need to model each message flow to compute its maximum arrival curve, and the behavior of each crossed node. These models are detailed in the next sections.

C. Traffic Model

To replace the current avionics backup network with the proposed UWB-based network, each data generated by an avionic application is encapsulated in an UWB frame, which defines the source and destination addresses. Afterwards, we consider that any aggregate traffic flow f_i^k generated by an end-system k consists of n_i periodic (or sporadic) subflows $f_{i,j}^k$, where $1 \leq j \leq n_i$, and belongs to a traffic class TC_i. TC_i is characterized by a tuple (T_i, Dl_i, L_i, e_i) for period (or minimum inter-arrival time for sporadic flow), deadline (equal to T_i unless otherwise explicitly specified), frame size integrating the protocol overhead and delivery time (i.e., $e_i = L_i/B$ where B is the medium transmission capacity), respectively. The

[1] $]s,t]$ is called backlogged period if $R(\tau) - R^*(\tau) > 0, \forall \tau \in]s,t]$

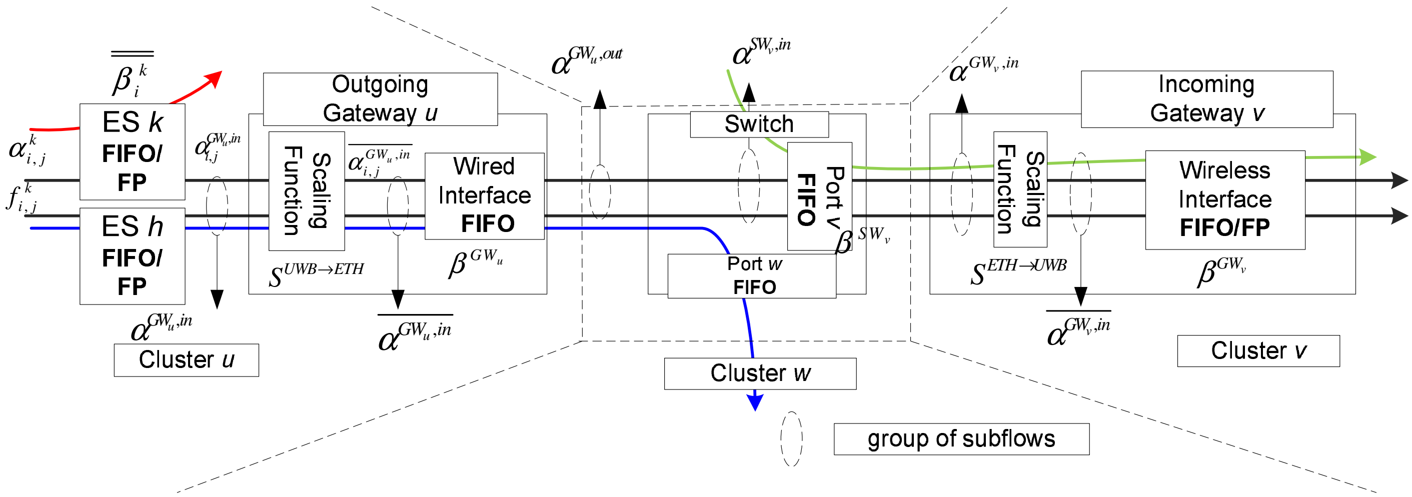

Figure 3: Flow Paths

arrival curve of aggregate traffic flow f_i^k, based on a packetized model, is given by:

$$\alpha_i^k(t) = \sum_{j=1}^{n_i} \alpha_{i,j}^k(t) = n_i L_i \lceil \frac{t}{T_i} \rceil \quad (1)$$

D. Refined End-Systems and TDMA Protocol Models using ILP

The considered end-systems generate messages independently and transmit their generated traffic flows on the shared medium based on the TDMA protocol under FIFO and FP policies. The classic service curve for a fluid flow model when a FIFO policy is implemented in end-system k has the following analytical expression:

$$\beta_{c,s^k}(t) = B \max(\lfloor \frac{t}{c} \rfloor s^k, t - \lceil \frac{t}{c} \rceil (c - s^k)), \forall t \geq 0 \quad (2)$$

where B is the medium transmission capacity, c is the TDMA cycle duration and s^k is the allocated slot to end-system k.

The main idea is based on the fact that an end-system k with a time slot s^k may not have access to the shared network during at maximum $c - s^k$. After this maximum duration, the end-system has exclusive access to the medium during its time slot s^k to transmit with medium transmission capacity B. When considering FP policy, each traffic flow will be transmitted before all lower priority flows and after all higher priority flows. Consider N aggregate traffic flows $f_1^k, .., f_N^k$ where f_i^k has higher priority than f_j^k if $i < j$. The residual service curve offered to traffic flow f_i^k, using Theorem 1 in Network Calculus, has the following analytical expression:

$$\beta_i^k(t) = (\beta_{c,s^k}^k(t) - \sum_{j=1}^{i-1} \alpha_j^k(t))_\uparrow \quad (3)$$

In [6], we proposed extended Network Calculus models to integrate the impact of non-preemption of message transmission under FIFO and FP policies. The associated service curves are explicitly defined in Theorems 2 and 3, respectively. The detailed proofs of these theorems are given in [4].

Theorem 2. *Consider an end-system k having a lower bound of offered time slot $\overline{s^k}$, generating N traffic flows where $e_{max} = \max_{1\leq i \leq N} e_i$ and $e_{min} = \min_{1 \leq i \leq N} e_i$, and implementing a FIFO policy. The offered* strict *service curve when considering non-preemptive message transmission is:*

$$\overline{\beta^k}(t) = \beta_{c,\overline{s^k}}(t - WT^k + (c - \overline{s^k})), \forall t \geq 0$$

where

$$WT^k = e_{max} + c - s^k,$$

and

$$\overline{s^k} = \begin{cases} \lfloor \frac{s^k}{e} \rfloor e & \text{if } e_{max} = e_{min} = e \\ \max\{s^k - e_{max}, e_{min}\} & \text{Otherwise} \end{cases}$$

Theorem 3. *Consider an aggregate traffic flow $f_{\leq i}^k$, including traffic flows $f_1^k,..., f_i^k$ with priorities higher or equal to i where $e_{max}^{1\leq j \leq i} = \max_{1 \leq j \leq i} e_j$ and $e_{min}^{1 \leq j \leq i} = \min_{1 \leq j \leq i} e_j$, and having a lower bound of offered TDMA time slot $\overline{s_{\leq i}^k}$, transmitted by the end-system* k *implementing FP policy. The* strict *service curve guaranteed to $f_{\leq i}^k$ when considering non-preemption feature is:*

$$\overline{\beta_{\leq i}^k(t)} = \beta_{c,\overline{s_{\leq i}^k}}(t - WT_{\leq i}^k + (c - \overline{s_{\leq i}^k})), \forall t \geq 0 \quad (4)$$

where

$$WT_{\leq i}^k = \min(e_{max}^{i<j\leq N} + e_{max}^{1\leq j \leq i} + c - s^k, c)$$

and

$$\overline{s_{\leq i}^k} = \begin{cases} \lfloor \frac{s^k}{e} \rfloor e & \text{if } e_{max}^{1\leq j\leq i} = e_{min}^{1 \leq j \leq i} = e \\ \max(e_{min}^{1\leq j \leq i}, s^k - e_{max}^{1 \leq j \leq i}) & \text{Otherwise} \end{cases}$$

Using Theorems 1 and 3, the residual service curve offered to the aggregate flow f_i^k is:

$$\overline{\beta_i^k}(t) = (\beta_{c,\overline{s_{\leq i}^k}}(t - WT_{\leq i}^k + (c - \overline{s_{\leq i}^k})) - \sum_{j=1}^{i-1} \alpha_j^k(t))_\uparrow \quad (5)$$

To compute tighter upper bounds on delay, we refine in this paper these service curves under the different policies based on ILP. First, analytical formulations of the optimization problems corresponding to the service policies are detailed. Then, the obtained parameters are integrated in the refined service curves.

For an end-system k generating N aggregate traffic flows, we consider x_i as the number of aggregate traffic flows that can be transmitted within a slot s^k. The respective ILP problem is as follows:

minimize

$$\overline{\overline{s^k}} = \sum_{i=1}^{N} x_i * e_i \quad (6)$$

subject to:

$$\sum_{i=1}^{N} x_i * e_i \leq s^k \quad (6a)$$

$$s^k - (\sum_{i=1}^{N} x_i * e_i) < e_{max} \quad (6b)$$

$$x_i \in \mathbb{N}, 1 \leq i \leq N \quad (6c)$$

where

- the objective is to minimize the offered TDMA time slot, and consequently maximize the remaining time and cover the worst-case scenario;
- constraint (6a) guarantees that the offered TDMA time slot $\overline{\overline{s^k}}$ is smaller than the allocated TDMA time slot s^k;
- constraint (6b) guarantees that the remaining time with the minimum offered TDMA time slot is smaller than the maximum message delivery time e_{max};
- constraint (6c) guarantees that the number of transmitted messages x_i of each traffic flow f_i^k is a nonnegative integer.

The minimum offered TDMA time slot that results from this ILP problem, $\overline{\overline{s^k}}$, is then integrated in the extended service curve defined in Th. 2 to obtain the refined service curve model, detailed in the following corollary.

Corollary 1. *Consider an end-system k having the minimum offered TDMA time slot $\overline{\overline{s^k}}$. A refined strict service curve guaranteed on TDMA-based network under FIFO multiplexing is*

$$\overline{\overline{\beta^k}}(t) = \beta_{c,\overline{\overline{s^k}}}(t - WT^k + (c - \overline{\overline{s^k}})) \quad (7)$$

This ILP formulation can be easily extended under a FP policy. To find the minimum offered TDMA time slot $\overline{\overline{s_{\leq i}^k}}$ of the aggregate flow $f_{\leq i}^k$, we need to consider only the subset of aggregate traffic flows $\{f_1^k, f_2^k, .., f_i^k\}$ instead of all traffic flows N in the ILP problem formulation (6). The obtained minimum offered slot $\overline{\overline{s_{\leq i}^k}}$ is then integrated in the extended service curve defined in Theorem 3 to obtain the refined service curve, detailed in the following corollary.

Corollary 2. *Consider an aggregate flow $f_{\leq i}^k$ having the minimum offered TDMA time slot $\overline{\overline{s_{\leq i}^k}}$. A refined strict service curve guaranteed on TDMA-based network under FP multiplexing is*

$$\overline{\overline{\beta_{\leq i}^k}}(t) = \beta_{c,\overline{\overline{s_{\leq i}^k}}}(t - WT_{\leq i}^k + (c - \overline{\overline{s_{\leq i}^k}})) \quad (8)$$

Using Theorem 1 and Corollary 2, a refined service curve for the aggregate flow f_i^k is given by:

$$\overline{\overline{\beta_i^k}}(t) = (\overline{\overline{\beta_{\leq i}^k}}(t) - \sum_{j=1}^{i-1} \alpha_j^k(t))_\uparrow \quad (9)$$

The optimization problem can be seen as a bin-packing problem which is known to be NP-hard. However, from a practical point of view, if the number of traffic flows is not too large (< 100), we can solve this optimization problem efficiently in a short time.

The delay bounds imposed by the end-system k to each subflow $f_{i,j}^k$ belonging to the aggregate traffic flow f_i^k, can be computed as the maximum horizontal distance between the associated arrival curve and the minimum service curve guaranteed by each end-system under FIFO or FP, and they are defined as following:

- with FIFO policy, using Eqs. 1 and 7, $\forall f_{i,j}^k$

$$D_{i,j}^{ES_k} = h(\alpha^k, \overline{\overline{\beta^k}}) \text{ where } \alpha^k(t) = \sum_{i=1}^{N} \alpha_i^k(t) \quad (10)$$

- with FP policy, using Eqs. 1 and 9, $\forall f_{i,j}^k$

$$D_{i,j}^{ES_k} = h(\alpha_i^k, \overline{\overline{\beta_i^k}}) \quad (11)$$

E. Outgoing Gateway Model

The outgoing gateway associated with cluster u performs two tasks: (i) encapsulate the UWB frame into the Giga Ethernet frame, (ii) perform the FIFO scheduling for the encapsulated Ethernet frames and forward them to the Gigabit Ethernet switch.

First, the arrival curve at the input of this gateway is the sum of output arrival curves of subflows in S_{GW_u}, which is the set of all subflows generated by any end-system k in cluster u and transmitted to the outgoing gateway GW_u; and it is as follows:

$$\begin{aligned} \alpha^{GW_u,in}(t) &= \min\{\sum_{f_{i,j}^k \in S_{GW_u}} \alpha_{i,j}^{GW_u,in}(t), Bt\} \\ &= \min\{\sum_{f_{i,j}^k \in S_{GW_u}} \alpha_{i,j}^{ES_k,out}(t), Bt\} \quad (12) \end{aligned}$$

where B is the maximum transmission capacity of the wireless link, and $\alpha_{i,j}^{ES_k,out}$ is the arrival curve of the subflow $f_{i,j}^k$ at the output of the end-system k. This latter is defined as $\alpha_{i,j}^{ES_k,out}(t) = \alpha_{i,j}^k(t + D_{i,j}^{ES_k})$ using Eqs. 1, 10 and 11.

Then, each received UWB packet from cluster u at the outgoing gateway GW_u is encapsulated in an Ethernet frame. Consequently, the amount of input traffic is scaled and then transmitted to the wired interface of GW_u. To model this function, we use the concept of an upper scaling curve, defined in [7], which is a wide sense increasing function, $\overline{S}$, that maps any amount of data a to $\overline{S}(a)$. It is easy to verify that the corresponding scaling curve of any subflow $f_{i,j}^k$ is:

$$\overline{S_{i,j}^{GW_u,k}}(a) = \frac{L_i^{ETH}}{L_i^{UWB}} a \tag{13}$$

where L_i^{ETH} and L_i^{UWB} are the lengths of Ethernet and UWB frames of $f_{i,j}^k$, respectively. Hence, the input arrival curve at the wired interface of the outgoing gateway GW_u, after the scaling process and using Eqs. 12 and 13, is:

$$\begin{aligned} \overline{\alpha^{GW_u,in}}(t) &= \min\{\sum_{f_{i,j}^k \in S_{GW_u}} \overline{\alpha_{i,j}^{GW_u,in}}(t)), B^S t\} \\ &= \min\{\sum_{f_{i,j}^k \in S_{GW_u}} \overline{S_{i,j}^{GW_u,k}}(\alpha_{i,j}^{ES_k,out}(t)), B^S t\} \end{aligned} \tag{14}$$

where

$$B^S = \max_i \frac{L_i^{ETH}}{L_i^{UWB}} B \tag{15}$$

On the other hand, the service curve offered by the gateway GW_u, implementing FIFO is:

$$\beta^{GW_u}(t) = Ct - \max_{f_{i,j}^k \in S_{GW_u}} L_i^{ETH} \tag{16}$$

where C is the transmission capacity of the Ethernet switch.

Hence, the delay bound imposed by the gateway GW_u to any subflow $f_{i,j}^k \in S_{GW_u}$, based on Eqs. 14 and 16, is:

$$D_{i,j}^{GW_u,k} = D^{GW_u} = h(\overline{\alpha^{GW_u,in}}, \beta^{GW_u}) \tag{17}$$

F. Switch Model

The Giga Ethernet switch will forward incoming packets from the different outgoing gateways to the corresponding output port of the switch according to FIFO. The input arrival curve of the output port of the switch, associated with the incoming gateway GW_v of cluster v, is the sum of output arrival curves of subflows in S_{SW_v}, which is the set of all subflows transmitted by any outgoing gateway GW_u to the output port of the switch associated with incoming gateway GW_v of cluster v, and it is as follows:

$$\alpha^{SW_v,in}(t) = \sum_{f_{i,j}^k \in S_{SW_v}} \alpha_{i,j}^{GW_u,out}(t) \tag{18}$$

where $\alpha_{i,j}^{GW_u,out}(t) = \overline{\alpha_{i,j}^{GW_u,in}}(t + D_{i,j}^{GW_u,k})$, using Eqs. 14 and 17.

The service curve of output port SW_v of the switch offered to this input traffic, under FIFO, is:

$$\beta^{SW_v}(t) = Ct - \max_{f_{i,j}^k \in S_{SW_v}} L_i^{ETH} \tag{19}$$

where C is the transmission capacity of the Ethernet switch.

Hence, the delay bound imposed by output port SW_v of the switch to any subflow $f_{i,j}^k \in S_{SW_v}$, using Eqs. 18 and 19, is as follows:

$$D_{i,j}^{SW_v,k} = D^{SW_v} = h(\alpha^{SW_v,in}, \beta^{SW_v}) \tag{20}$$

G. Incoming Gateway Model

Incoming gateway GW_v associated with cluster v decapsulates any received Ethernet frame to obtain the original UWB frame, the gateway then transmits the obtained frames according to the TDMA protocol under FIFO or FP policies, as any end-system in cluster v. The input arrival curve at GW_v is the sum of output arrival curves of subflows in S_{SW_v}, and it is as follows by using Eqs. 18 and 20:

$$\begin{aligned} \alpha^{GW_v,in}(t) &= \min\{\sum_{f_{i,j}^k \in S_{SW_v}} \alpha_{i,j}^{SW_v,out}(t), Ct\} \\ &= \min\{\alpha^{SW_v,out}(t), Ct\} \\ &= \min\{\alpha^{SW_v,in}(t + D^{SW_v}), Ct\} \end{aligned} \tag{21}$$

As the outgoing gateway, the amount of input traffic is scaled and then transmitted to the wireless interface of GW_v. Consequently, the corresponding scaling curve of any subflow $f_{i,j}^k$ is:

$$\overline{S_{i,j}^{GW_v,k}}(a) = \frac{L_i^{UWB}}{L_i^{ETH}} a \tag{22}$$

Hence, the input arrival curve at the wireless interface of the incoming gateway GW_v after the scaling process, using Eq. 21, is:

$$\begin{aligned} \overline{\alpha^{GW_v,in}}(t) &= \min\{\sum_{f_{i,j}^k \in S_{SW_v}} \overline{\alpha_{i,j}^{GW_v,in}}(t)), C^S t\} \\ &= \min\{\sum_{f_{i,j}^k \in S_{SW_v}} \overline{S_{i,j}^{GW_v,k}}(\alpha_{i,j}^{SW_v,out}(t)), C^S t\} \end{aligned} \tag{23}$$

where C^S is the scaling switch capacity and given by:

$$C^S = \max_i \frac{L_i^{UWB}}{L_i^{ETH}} C \tag{24}$$

Similarly, the input arrival curve of traffic class TC_i at the wireless interface of the incoming gateway GW_v after the scaling process is given by:

$$\overline{\alpha_i^{GW_v,in}}(t) = \min\{\sum_{f_{i,j}^k \in S_{SW_u,i}} \overline{S_{i,j}^{GW_v,k}}(\alpha_{i,j}^{SW_v,out}(t)), C_i^S t\} \tag{25}$$

where $C_i^S = \frac{L_i^{UWB}}{L_i^{ETH}} C$ and $S_{SW_u,i}$ is the set of all subflows in S_{SW_u} and belonging to TC_i.

Therefore, the delay bound imposed by the incoming gateway GW_v to any subflow $f_{i,j}^k \in S_{SW_v}$ is as follows:

- Under FIFO, using Corollary 1 and Eq. 23,

$$D_{i,j}^{GW_v,k} = D^{GW_v} = h(\overline{\alpha^{GW_v,in}}, \overline{\overline{\beta^{GW_v}}}) \tag{26}$$

- Under FP, using Corollary 2 and Eqs. 9 and 25,

$$D_{i,j}^{GW_v,k} = D_i^{GW_v} = h(\overline{\alpha_i^{GW_v,in}}, \overline{\overline{\beta_i^{GW_v}}}) \tag{27}$$

V. Upper Bounds on End-to-End Delays

In this section, we detail the end-to-end delay bounds of intra-cluster and inter-cluster traffic by integrating the effect of the reliability mechanisms. Then, some numerical results are illustrated to show the impact of the refined models on delays, with reference to the extended models detailed in [6]

A. Impact of Reliability Mechanisms

As described in Section III-C, to guarantee the required PER level of avionic applications, PER_L, we consider time and frequency diversity mechanisms to enhance the offered PER of UWB technology, PER_{UWB}. To conduct timing analysis of such a network, we need to integrate the impact of reliability mechanisms which certainly will increase the offered reliability level but at the same time increase the end-to-end delay bounds.

We consider η_f the number of frequency channels due to frequency diversity mechanism, and η_t the number of packet transmissions on each frequency channel due to a time diversity mechanism. Consequently, if the two diversity mechanisms are combined, then each message is transmitted $\eta_f \times \eta_t$ times. Hence, the offered PER of such a network is equal to $PER_{UWB}^{\eta_f \times \eta_t}$, and the avionic reliability requirement is guaranteed if the following condition is verified:

$$PER_{UWB}^{\eta_f \times \eta_t} \leq PER_L \tag{28}$$

Hence, the following conditions has to be verified:

$$\eta_t \geq \lceil \frac{log_{PER_{UWB}}(PER_L)}{\eta_f} \rceil \tag{29}$$

Increasing the number of transmissions of the same message leads to increasing the quantity of traffic generated by each end-system and consequently the associated maximum arrival curve. The decorrelated η_f frequency channels can be modeled as η_f redundant wireless links, and on each considered wireless link there are η_t copies of the same generated message by any end-system.

B. Computing End-to-End Delay Bounds

To integrate the impact of reliability mechanisms, the delay bounds imposed by the end-system k, computed in Eq. 10 and 11, are updated as following.

- with FIFO policy, $\forall f_{i,j}^k$

$$D_{i,j}^{ES_k} = h(\eta_t.\alpha^k, \overline{\overline{\beta^k}}) \tag{30}$$

- with FP policy, $\forall f_{i,j}^k$

$$D_{i,j}^{ES_k} = h(\eta_t.\alpha_i^k, \overline{\overline{\beta_i^k}}) \tag{31}$$

Similarly, the delay bounds for incoming gateway v in Eqs 26, 27 have to be updated by considering η_t copies of each forwarded packet.

The delay bounds in outgoing gateway v and switch are not affected by the diversity techniques because only one correct copy of each packet will be forwarded. Hence, the end-to-end delay bounds for intra-cluster and inter-cluster traffic are as follows:

- for intra-cluster traffic, for any aggregate flow f_i^k in cluster u:
$$D_i^{eed} = D_i^u = \max_{\forall f_{i,j}^k} D_{i,j}^{ES_k} \tag{32}$$
- for inter-cluster traffic, for any aggregate flow f_i^k transmitted from cluster u to cluster v:
$$D_i^{eed} = \max_{\forall (u,v)} D_i^{u \to v} = D_i^u + D^{GW_u} + D^{SW_v} + D_i^{GW_v} \tag{33}$$

C. Numerical Results

We consider an example avionics cluster supporting 10 end-systems and two traffic classes TC_1, TC_2 with deadlines 8ms and 16ms, respectively. We fix the $PER = 10^{-3}$ and increase the bandwidth utilization of the network. The end-to end delays are computed under FIFO and FP, using extended and refined models proposed in [6] and in this paper, respectively. Results are illustrated in Figs. 4 and 5, respectively. The results show the enhancement of the delay bounds obtained with the refined models using ILP, compared with the extended models. Particularly, under FIFO, for $n_f = 2$ and a bandwidth utilization 19%, the extended model leads to delay bounds greater than the shortest deadline (8ms) and consequently cannot guarantee the system schedulability, unlike the refined model. Furthermore, we have the same result under FP for TC_2 when $n_f = 4$ and the bandwidth utilization is 57%. It is worth to note that the delay bounds for TC_1 are the same with extended and refined models due to $\overline{s_{\leq 1}^k} = \overline{\overline{s_{\leq 1}^k}} = \lfloor \frac{s^k}{e_1} \rfloor e_1 \forall k$. These results show the importance of the used model to verify the system schedulability, and the interest of using refined model to improve system schedulability compared with the extended one.

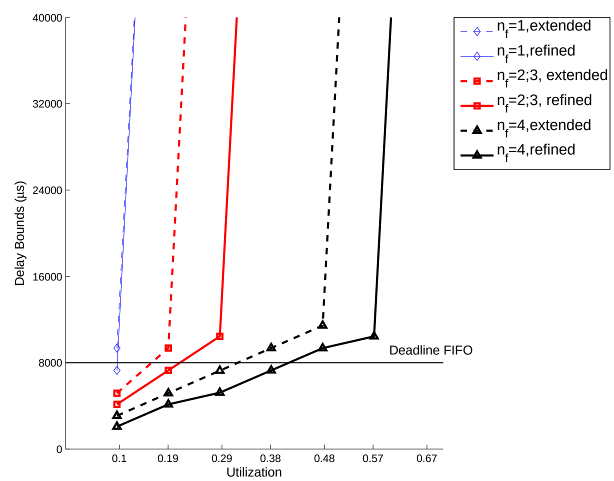

Figure 4: Extended vs Refined models delay bounds under FIFO

VI. Optimal TDMA Cycle Length

In this section, we present the problem formulation to find the optimal cycle duration which minimizes the delays. Then, the optimization approach to solve the problem is detailed.

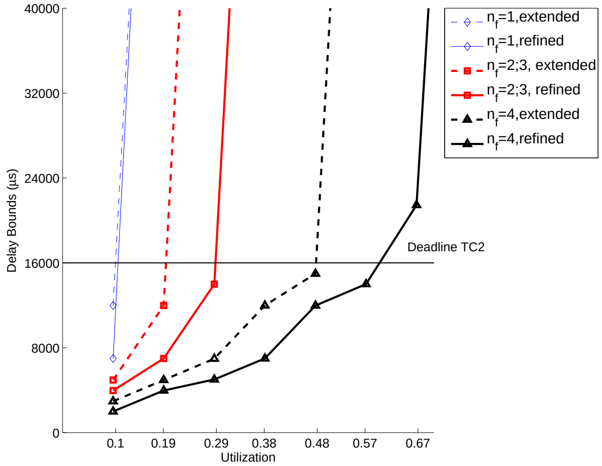

Figure 5: Extended vs Refined models delay bounds for TC_2 under FP

A. Problem Formulation

The aim is to find the optimal TDMA cycle duration and slot allocation for the different avionic clusters to guarantee the system schedulability, and to minimize the upper bounds on delays of each traffic flow. We can formulate the optimization problem, using Eqs. 32 and 33, as follows:

$$\begin{aligned} \underset{\forall u,(c^u,s^{1,u},s^{2,u},\ldots,s^{M,u})}{\text{minimize}} \quad & D_i^{eed}, \forall i=1,2,\ldots,N \\ \text{subject to} \quad & D_i^{eed} \leq Dl_i,\ i=1,\ldots,N. \end{aligned} \tag{34}$$

This is a non-linear multi-criteria optimization problem in the general case. Therefore, to simplify this problem, we will transform it to a mono-criteria optimization problem. Under FIFO, we consider as an objective function

$$D = \max_i D_i^{eed} \tag{35}$$

However, under FP, we allocate a weight w_i to each criteria to have as an objective function:

$$D = \sum_{i=1}^{N} w_i D_i^{eed} \tag{36}$$

where $w_i = \dfrac{1}{Dl_i}$ which guarantees that if $Dl_i < Dl_j$, then $w_i > w_j$.

To solve this problem, we reduce the number of variables by using the *traffic proportional slot sizing* (TPSS) as [8] for slot allocation, i.e., to allocate to each end-system a slot proportional to its generated rate. Hence, the only variable to optimize is the cycle duration c^u for each cluster u. The optimization is then reformulated as follows:

$$\begin{aligned} \underset{\forall u,c^u}{\text{minimize}} \quad & D \\ \text{subject to} \quad & D_i^{eed} \leq Dl_i, \forall 1 \leq i \leq N \end{aligned} \tag{37}$$

B. Optimization Algorithm

The following algorithm is used to find the optimal cycle duration for each cluster that minimizes the delay bounds and respects the system's schedulability.

Step 1: For each cluster u, we consider:

$$min\_cycle(u) = t_{syn} + \sum_{\forall k \in clt_u} \max_{f_i^k} e_i \tag{38}$$

$$max\_cycle(u) = \min_i Dl_i, \tag{39}$$

where clt_u is the set of all end-systems in cluster u.

Step 2: For each cluster u, we build the set $\mathscr{C}^u$ of all TDMA cycle durations in $[min\_cycle(u), max\_cycle(u)]$ as follows:

for $i := \lceil \frac{min\_cycle(u)}{q_c} \rceil$ **to** $\lfloor \frac{max\_cycle(u)}{q_c} \rfloor$ **do**
$c^u \leftarrow q_c.i$
$\mathscr{C}^u \leftarrow \mathscr{C}^u \cup c^u$
end for

where q_c corresponds to a sampling step.

Step 3: Consider $\mathscr{M}$ clusters, for each configuration $\{c^1, c^2, \ldots, c^{\mathscr{M}}\}$ in $\mathscr{C}^1 \times \mathscr{C}^2 \times \ldots \times \mathscr{C}^{\mathscr{M}}$, we apply TPSS for slots allocation in each cluster c^u. Then, we compute the end-to-end delay bound D_i^{eed} for each traffic class TC_i to verify the schedulability constraint.

Step 4: Among all the schedulable configurations, we select the one minimizing the objective function, which is considered as the optimal configuration.

VII. Avionic Case Study

A. Description

In this section, we consider a representative avionic case study consisting of $N = 52$ end-systems and supporting three traffic classes described in Tab. I. The offered PER by UWB technology is fixed as $PER_{UWB} = 10^{-3}$, and the PER level is equal to $PER_L = 10^{-10}$. We consider a network topology based on two clusters 1 and 2, which correspond to the main and upper avionics bays of Airbus A380. There are 36 and 16 end-systems in clusters 1 and 2, respectively. Tab. II represents the configuration of these two clusters.

Our main objective is to find the optimal TDMA cycle durations for the avionics clusters, which minimize the delay bounds while respecting the system schedulability under FIFO and FP policies.

Table I: Parameters of Traffic Classes

	T (μs)	Dl (μs)	Payload (Byte)	Transmission time (μs)
TC_1	4000	4000	482	33
TC_2	16000	16000	288	25
TC_3	32000	32000	16	14

Table II: Configuration of Clusters 1 and 2

Traffic Class	Intra-cluster			Inter-cluster	
	TC_1	TC_2	TC_3	TC_2	TC_3
Num of flows in Cluster 1	18	37	56	32	55
Num of flows in Cluster 2	10	15	20	7	10

B. Performance Analysis

To highlight the impact of the cycle duration on system performance, end-to-end delay bounds are computed under two configurations. The first one corresponds to a default configuration where the TDMA cycle durations are $c^1 = c^2 = \min_i Dl_i =$

4ms. The second one corresponds to the configuration where TDMA cycle durations are computed based on the described optimization algorithm in Section VI-B with $q_c = 50\ \mu$s. The optimal TDMA cycles under FIFO and FP for each cluster are shown in Tabs III and IV.

Under FIFO in the end-systems and the incoming gateways, the number of frequency channels is varied, $n_f = 1,2,3,4$, and the computed end-to-end delay bounds are shown in Tab. III. As we can notice, the end-to-end delay bounds with default configuration are greater than the ones with optimized configuration. The delay bounds of traffic classes are infinite when $n_f = 1$, and particularly greater than the deadlines when $n_f = 2,3$ for TC_1 and TC_2. Furthermore, the system schedulability is only achieved with $n_f = 4$.

Table III: End-to-end delay bounds under FIFO

	n_f	TC_1 (μs)	TC_2 (μs)	TC_3 (μs)	c^1 (μs)	c^2 (μs)
Default config.	2,3	7878	30556	31845	4000	4000
Optimized config.	2,3	7782	28422	28439	3950	3100
Default config.	4	3939	15829	15870	4000	4000
Optimized config.	4	3296	13796	13805	3150	1100

Table IV: End-to-end delay bounds under FP

	n_f	TC_1 (μs)	TC_2 (μs)	TC_3 (μs)	c_1 (μs)	c_2 (μs)
Default config.	2,3	3972	15917	35866	4000	4000
Optimized config.	2,3	3924	13944	31844	3950	3050
Default config.	4	3939	7971	15870	4000	4000
Optimized config.	4	1676	7288	15392	1650	1200

Under FP in the end-systems and incoming gateways, the end-to-end delay bounds obtained under the two configurations and with different frequency numbers are shown in Tab. IV. We can notice that the system is schedulable with optimized configuration under FP where $n_f = 2$, unlike under FIFO where $n_f = 4$ was needed. Hence, these results show the importance of TDMA cycle duration selection to enhance the system's performance, and particularly delay bounds and reliability level.

VIII. Conclusion

A UWB-based network has been proposed as an alternative backup network for avionic applications to reduce weight and consequently decrease costs and maintenance for new generation aircraft. The analysis and performance optimization of such a proposal were conducted. First, a refined timing analysis, based on Network Calculus and ILP approach, was detailed under FIFO and FP policies and in an error-prone environment to compute end-to-end delay bounds. Then, TDMA cycle duration was optimized to minimize the delay bounds while respecting the system's schedulability. Results for a representative avionic case study show the efficiency of our timing and optimization approaches to enhance the system's performance in terms of schedulability and reliability.

The performance optimization of such a proposal in terms of reliability mechanisms overhead, by integrating ARQ mechanisms and using Stochastic Network Calculus analysis, is an on-going work.

References

[1] W. Alliance. ECMA-368 High Rate Ultra Wideband PHY and MAC Standard. ECMA Std., 2008.

[2] A. Bouillard, L. Jouhet, E. Thierry, et al. Service curves in network calculus: dos and don'ts. 2009.

[3] A. Bouillard and G. Stea. Exact worst-case delay for FIFO-multiplexing tandems. In *ValueTools*, Torino, Italy, 2012.

[4] D.-K. Dang and A. Mifdaoui. Timing Analysis of TDMA-based Networks using Network Calculus and Integer Linear Programming. In *MASCOTS*, Paris, France, 2014.

[5] D.-K. Dang, A. Mifdaoui, and T. Gayraud. Fly-By-Wireless for next generation aircraft: Challenges and potential solutions. In *IFIP Wireless Day (WD)*, Dublin, Ireland, 2012.

[6] D.-K. Dang, A. Mifdaoui, and T. Gayraud. Design and Analysis of UWB-based Network for Reliable and Timely Communications in Safety-Critical Avionics. In *WFCS*, Toulouse, France, 2014.

[7] M. Fidler and J. B. Schmitt. On the way to a distributed systems calculus: An end-to-end network calculus with data scaling. In *ACM SIGMETRICS Performance Evaluation Review*, volume 34, 2006.

[8] N. Gollan and J. Schmitt. Energy-Efficent TDMA Design Under Real-Time Constraints in Wireless Sensor Networks. In *MASCOTS*, Istanbul, Turkey, 2007.

[9] A. Koubâa, M. Alves, E. Tovar, and A. Cunha. An implicit GTS allocation mechanism in IEEE 802.15.4 for time-sensitive wireless sensor networks: theory and practice. *Real-Time Systems*, 39, 2008.

[10] J. Le Boudec and P. Thiran. *Network calculus: a theory of deterministic queuing systems for the internet*. Springer-Verlag, 2001.

[11] X. C. Tong. *Advanced materials and design for electromagnetic interference shielding*. CRC Press, 2008.

[12] E. Wandeler and L. Thiele. Optimal TDMA time slot and cycle length allocation for hard real-time systems. In *ASP-DAC*, Yokohama, Japan, 2006.